

Reactions of Hydrotris(pyrazolyl)borate (Tp)-Supported Ruthenium Dihydrogen Complexes $[\text{TpRu}(\text{L}_2)(\text{H}_2)]^+$ ($\text{L}_2 = \text{dppm}, \text{dppp}, (\text{PPh}_3)_2$) with O_2

Man Lok Man,[†] Jun Zhu,[‡] Siu Man Ng,[†] Zhongyuan Zhou,[†] Chuanqi Yin,[†] Zhenyang Lin,^{*,‡} and Chak Po Lau^{*,†}

Department of Applied Biology & Chemical Technology, The Hong Kong Polytechnic University, Hung Hom, Kowloon, Hong Kong, China, and Department of Chemistry, The Hong Kong University of Science and Technology, Clear Water Bay, Kowloon, Hong Kong, China

Received August 2, 2004

The η^2 -dihydrogen complex $[\text{TpRu}(\text{L}_2)(\text{H}_2)]^+$ ($\text{L}_2 = \text{dppm}, \text{dppp}, \text{or } (\text{PPh}_3)_2$) prepared in situ by protonation of the hydride precursor reacts with O_2 to yield the paramagnetic Ru^{III} -superoxo complex $[\text{TpRu}^{\text{III}}(\text{L}_2)(\text{O}_2)]^+$, in which antiferromagnetic coupling between the Ru^{III} ion ($d^5, S = 1/2$) and the coordinated superoxide radical ($S = 1/2$) does not seem to be present. In THF, the superoxo moiety of the complex readily abstracts a hydrogen atom from the solvent to generate the hydroperoxo ($-\text{OOH}^-$) group, which then changes into the hydroxo ligand by transferring an oxygen atom to a phosphine ligand. Density functional theory calculation at the B3LYP level on the model complex $[\text{TpRu}(\text{PH}_3)_2(\text{O}_2)]^+$ shows that the Ru^{III} -superoxo(O_2^-) structure with a triplet state is more stable than the Ru^{IV} -peroxo(O_2^{2-}) structure with a singlet state by 5.2 kcal/mol. On the other hand, the analogous Cp model complex $[\text{CpRu}(\text{PH}_3)_2(\text{O}_2)]^+$ prefers the Ru^{IV} -peroxo(O_2^{2-}) structure over the Ru^{III} -superoxo(O_2^-) structure by 2.9 kcal/mol.

Introduction

The activation of oxygen by transition metals is of paramount importance in oxidative organic and biological reactions, and the transition metal– O_2 adduct is believed to play a crucial role in O_2 transport in biological systems.¹

Several ruthenium η^2 - O_2 complexes have been prepared by reacting the 16 e^- unsaturated Ru^{II} species with O_2 or by substitution of O_2 for labile ligands such as H_2 , N_2 , and weakly coordinated solvent molecule in saturated Ru^{II} complexes.² The X-ray structures of these complexes show that the O–O distances of the η^2 - O_2 ligands are approximately intermediate between the reported superoxide (1.28 Å in KO_2)³ and peroxide (1.49 Å in H_2O_2)⁴ distances, suggesting that these η^2 - O_2 complexes should be formally considered as Ru^{IV} com-

plexes. Jia et al. reported that upon exposing an equilibrium mixture of the dihydrogen complex and dihydride species, $[\text{Cp}^*\text{Ru}(\text{dppm})(\text{H}_2)]^+ - [\text{Cp}^*\text{Ru}(\text{dppm})\text{H}_2]^+$ to air, the former reacts with O_2 by simple ligand displacement to give the η^2 -peroxo complex $[\text{Cp}^*\text{Ru}(\text{dppm})(\eta^2\text{-O}_2)]^+$; for the dihydride complex, it is proposed that O_2 inserts into one of the hydride ligands, forming the hydroperoxide, which then oxidizes one of the phosphine arms of dppm to give phosphine oxide by O-transfer.⁵ In their attempt to synthesize ruthenium dioxygen complexes bearing the Tp^{iPr} ligand ($\text{Tp}^{\text{iPr}} = \text{hydrotris}(3,5\text{-diisopropylpyrazolyl})\text{borate}$) by reacting the unsaturated cationic ruthenium(II) species $[\text{Tp}^{\text{iPr}}\text{Ru}(\text{diphosphine})]^+$ with O_2 , Akita, Moro-oka, and co-workers did not obtain the desired products, but instead obtained different products resulting from different types of oxygenation reactions, depending on the structures of the diphosphine ligands. One of the reactions involves a novel oxidative $\text{C}(\text{sp}^3) - \text{C}(\text{sp}^3)$ bond cleavage.⁶ We here report our work on the reactions of ruthenium dihydrogen complexes $[\text{TpRu}(\text{L}_2)(\text{H}_2)]\text{BF}_4$ ($\text{Tp} = \text{hydrotris}(\text{pyrazolyl})\text{borate}$; **1**, $\text{L}_2 = \text{dppm}$; **5**, $\text{L}_2 = \text{dppe}$; **9**, $\text{L}_2 = (\text{PPh}_3)_2$) with O_2 and show that the reactivities of these complexes toward O_2 are quite different from those of the Cp analogues, which usually undergo H_2/O_2 exchange with O_2 to yield the η^2 -peroxo complexes.

Results and Discussion

Reaction of $[\text{TpRu}(\text{dppm})(\text{H}_2)]\text{BF}_4$ (**1**) with O_2 in THF. Reacting the dihydrogen complex $[\text{TpRu}(\text{dppm})-$

(5) Jia, G.; Ng, W. S.; Chu, H. S.; Wong, W.-T.; Yu, N.-T.; Williams, I. D. *Organometallics* **1999**, *18*, 3597.

(6) Takahashi, Y.; Hikichi, S.; Akita, M.; Moro-oka, Y. *Chem. Commun.* **1999**, 1491.

* To whom correspondence should be addressed. (Z.L.) E-mail: chzlin@ust.hk. (C.P.L.) Fax: (852) 2364 9932. E-mail: bceplau@inet.polyu.edu.hk.

[†] The Hong Kong Polytechnic University.

[‡] The Hong Kong University of Science and Technology.

(1) (a) Martel, A. E.; Sawyer, D. T., Eds. *Oxygen Complexes and Oxygen Activation by Transition Metals*; Plenum Press: New York, 1988. (b) Thematic issue of *Chem. Rev.* (Metal-Dioxygen Complexes): *Chem. Rev.* **1994**, *94*, 567. (c) Sheldon, R. A.; Kochi, J. K. *Metal-Catalyzed Oxidations of Organic Compounds*; Academic Press: New York, 1981. (d) Akita, M.; Moro-oka, Y. *Catal. Today* **1998**, *44*, 183. (e) Murahashi, S. *Angew. Chem., Int. Ed. Engl.* **1995**, *34*, 2443.

(2) (a) Jiménez-Tenorio, M.; Puerta, M. C.; Valerga, P. *J. Am. Chem. Soc.* **1993**, *115*, 9794. (b) Jiménez-Tenorio, M.; Puerta, M. C.; Valerga, P. *Inorg. Chem.* **1994**, *33*, 3515. (c) Martelletti, A.; Gramlich, V.; Zürcher, F.; Mezzetti, A. *New J. Chem.* **1999**, 199. (d) Kirchner, K.; Mauthner, K.; Mereiter, K.; Schmid, R. *J. Chem. Soc., Chem. Commun.* **1993**, 892.

(3) Valentine, J. S. *Chem. Rev.* **1973**, *73*, 235.

(4) Savariault, J. M.; Lehmann, M. S. *J. Am. Chem. Soc.* **1980**, *102*, 1298.

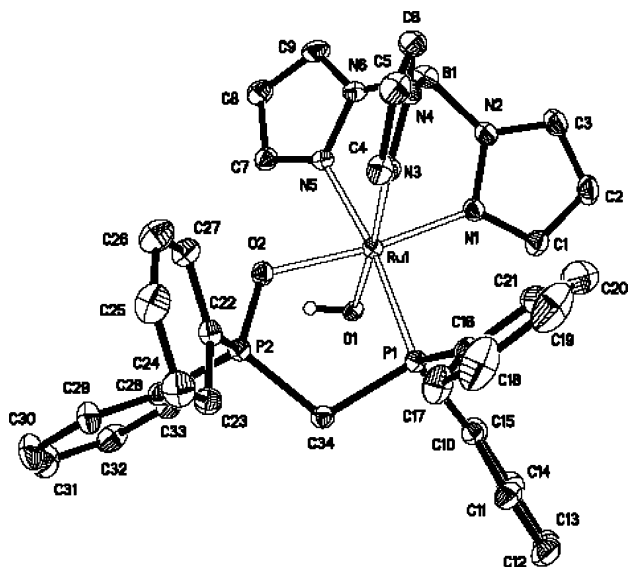


Figure 1. X-ray structure of $\{\text{TpRu}[\text{Ph}_2\text{PCH}_2\text{P}(\text{O})\text{Ph}_2](\text{OH})\}\text{BF}_4$ (**2**).

(H_2) BF_4 (**1**),⁷ prepared in situ by acidification of the hydride precursor $\text{TpRu}(\text{dppm})\text{H}^7$ with $\text{HBF}_4 \cdot \text{OEt}_2$ in THF, with O_2 (1 atm) for 3 h afforded, after removal of the solvent, a reddish brown solid. The ^1H and $^{31}\text{P}\{^1\text{H}\}$ NMR spectra of the solid were found to be identical to those of an authentic aquo complex, $[\text{TpRu}(\text{dppm})(\text{H}_2\text{O})]\text{BF}_4$ (**3**). Complex **3** is probably formed via displacement of the dihydrogen ligand of **1** by residual water in the solvent. Since an unusually concentrated solution of the reddish brown solid had to be used for the NMR measurements, we suspected that **3** might be a minor component of a solid, the major component of which is probably NMR silent. We therefore grew single crystals by layering of hexanes onto a CH_2Cl_2 solution of the solid, and an X-ray crystallographic study of a single crystal revealed its molecular structure to be that of the hydroxo species $[\text{TpRu}\{\text{Ph}_2\text{PCH}_2\text{P}(\text{=O})\text{Ph}_2\}(\text{OH})]\text{BF}_4$ (**2**). In this complex, one of the phosphine moieties of the dppm ligand is oxidized to the phosphine oxide and the metal center is Ru^{III} , which is paramagnetic. The molecular structure of the cation $[\text{TpRu}\{\text{Ph}_2\text{PCH}_2\text{P}(\text{=O})\text{Ph}_2\}(\text{OH})]^{2+}$ (**2**⁺) is shown in Figure 1. Crystal data and refinement details are given in Table 1. Selected bond distances and angles are given in Table 2. The $\text{Ru}-\text{OH}$ distance in **2**⁺, which measures 1.989(1) Å, is comparable to that in $[\text{Ru}(\eta^6\text{-C}_5\text{Me}_4\text{CH}_2)(\text{tmed})(\text{OH})]\text{BAR}'_4$ ($\text{BAR}'_4 = 3,5\text{-C}_6\text{H}_3(\text{CF}_3)_2$) ($\text{Ru}-\text{OH}$, 1.990(3) Å),⁸ but is short compared to the $\text{Ru}-\text{OH}$ distances reported for other ruthenium hydroxo complexes: 2.067(4) Å in $\text{Tp}^{\text{iPr}}\text{Ru}(\text{dppe})(\text{OH})$,⁹ 2.158(5) Å in $[\text{Tp}^{\text{iPr}}\text{Ru}(\text{dppe})(\text{OH})]\text{PF}_6$,⁶ 2.230(2) Å in *trans*- $[\text{Ru}(\text{DMPE})(\text{H})(\text{OH})\cdot\text{H}_2\text{O}]_2$.¹⁰ The phosphine oxide moiety is bonded to the metal, as evidenced by the $\text{Ru}-\text{O}$ distance of 2.060(1) Å. It is noted that the scorpionato arm trans to the phosphine oxide is bonded more tightly to the ruthenium than the one trans to the phosphine moiety ($\text{Ru}-\text{N}(1)$, 2.033(2)

Å vs $\text{Ru}-\text{N}(5)$, 2.107(1) Å), indicative of the smaller trans-influence of the phosphine oxide relative to that of the phosphine. Pure complex **2**, which was obtainable by recrystallization of the reddish brown solid from $\text{CH}_2\text{Cl}_2/\text{hexanes}$, was characterized using IR spectroscopy ($\nu(\text{Ru}-\text{OH})$ 3127 cm^{-1} (w), $\nu(\text{P}=\text{O})$ 1118 (sh)), ESI-MS (m/z , 732 for **2**⁺) spectroscopy, and elemental analysis. Pure **2** was found to be NMR silent. The relatively low O–H stretching frequency of **2** is a reflection of decreased electron density within the O–H bond; the highly electrophilic metal center withdraws electron density from the hydroxo group and reduces its bond strength. The deuterium-labeled complex $[\text{TpRu}\{\text{Ph}_2\text{PCH}_2\text{P}(\text{=O})\text{Ph}_2\}(\text{OD})]\text{BF}_4$ (**2-d**₁) was obtained when THF-d_8 was used in place of THF. **2-d**₁ showed the O–D stretching frequency at 2468 cm^{-1} and the O–H band basically disappeared. Obviously, the THF-d_8 was the deuterium source for the O–D bond of **2-d**₁.

Reaction of $[\text{TpRu}(\text{dppm})(\text{H}_2)]\text{BF}_4$ (1**) with O_2 in CH_2Cl_2 .** Changing the solvent from THF to dichloromethane gave a major product different from **2**. Thus, reacting a solution of **1**, prepared in situ by acidification of $\text{TpRu}(\text{dppm})\text{H}$ in CH_2Cl_2 with $\text{HBF}_4 \cdot \text{OEt}_2$, with oxygen at room temperature for 3 h yielded a red solid. After removing the minute amount of **3** from the solid by washing with diethyl ether and hexanes, the washed red solid was found to be NMR silent. Although several attempts to grow single crystals for X-ray diffraction analysis from the solutions of the red solid failed, IR spectroscopic study of the solid provided valuable information on its structure. The IR spectrum of the red solid shows a weak band at 1188 cm^{-1} . This band is in the region associated with the stretching of a superoxo (O_2^-) ligand. The shifted band of the isotopic $^{18}\text{O}_2^-$ ligand is unfortunately masked by the strong bands of the Tp and the phosphine ligands in the 1060–1140 cm^{-1} region. The ESI-MS of the solid displayed a parent peak at m/z 731, assignable to $[\text{TpRu}(\text{dppm})(\text{O}_2)]^+$; a peak at m/z 669 could be assigned to $[\text{TpRu}(\text{dppm})]^+$. We therefore propose that the reaction of the η^2 -dihydrogen complex **1** with O_2 in CH_2Cl_2 yields a superoxo ruthenium(III) complex, $[\text{TpRu}^{\text{III}}(\text{dppm})(\text{O}_2)]\text{BF}_4$ (**4**). We are unfortunately not able to know the bonding mode of the superoxo ligand in **4** in the absence of the X-ray structure. Akita, Moro-oka, and co-workers also suggested the intermediacy of the Ru^{III} -superoxo species in the reaction of $\text{Tp}^{\text{iPr}}\text{Ru}(\text{diphosphine})(\text{H}_2\text{O})^+$ with O_2 , but they have not been able to isolate or detect the superoxo intermediates.⁶ Noteworthy is the difference in the lability of the H_2O ligand in our Tp-Ru complex $[\text{TpRu}(\text{dppm})(\text{H}_2\text{O})]\text{BF}_4$ (**3**) and that in $[\text{Tp}^{\text{iPr}}\text{Ru}(\text{diphosphine})(\text{H}_2\text{O})]^+$. Complex **3** seems to be able to survive the attack by O_2 , but the water ligand in the Tp^{iPr} -supported complex is easily displaced by dioxygen.

The present Tp-ruthenium superoxo complex is unique because it is well known that the analogous cyclopentadienyl (Cp and Cp derivatives) and most of the other ruthenium(II) complexes react with O_2 to form $\eta^2\text{-O}_2$ complexes, in which the ruthenium centers are formally considered as Ru^{IV} and the dioxygen as a peroxo ligand (O_2^{2-}). The pentamethylcyclopentadienyl (Cp^*) ruthenium species with a diamine ligand might be considered as an exceptional case. It was postulated that coordination of dioxygen to the $16e^-$ species $[\text{Cp}^*\text{Ru}(\text{tmed})]^+$ first

(7) Chan, W. C.; Lau, C. P.; Chen, Y. Z.; Fan, Y. Q.; Ng, S. M.; Jia, G. *Organometallics* **1997**, *16*, 34.

(8) Gemel, C.; Mereiter, K.; Schmid, R.; Kirchner, K. *Organometallics* **1997**, *16*, 5601.

(9) Akita, M.; Takahashi, Y.; Hikichi, S.; Moro-oka, Y. *Inorg. Chem.* **2001**, *40*, 169.

(10) Burn, M. J.; Fickes, M. G.; Hartwig, J. G.; Hollander, F. J.; Bergman, R. G. *J. Am. Chem. Soc.* **1993**, *115*, 5875.

Table 1. Crystal Data and Structure Refinement for Complexes 2, 6, and 11

	2	6	11
empirical formula	Ru(OH)(C ₃₄ H ₃₂ BN ₆ P ₂ O)·BF ₄	Ru(OH)(C ₃₆ H ₃₆ BN ₆ OP ₂)·BF ₄ ·CH ₂ Cl ₂	Ru C ₂₇ H ₂₈ B ₂ F ₄ N ₆ O ₂ P
fw	818.29	931.27	698.21
temp	294(2) K	294(2) K	294(2) K
wavelength	0.71073 Å	0.71073 Å	0.71073 Å
cryst syst	monoclinic	monoclinic	tetragonal
space group	<i>P</i> 2(1)/ <i>n</i>	<i>P</i> 2(1)/ <i>n</i>	<i>P</i> 4(3)2(1)2
unit cell dimens	<i>a</i> = 10.9829(19) Å <i>α</i> = 90° <i>b</i> = 16.310(3) Å <i>β</i> = 93.715(4)° <i>c</i> = 20.237(4) Å <i>γ</i> = 90°	<i>a</i> = 15.394(2) Å <i>α</i> = 90° <i>b</i> = 15.884(2) Å <i>β</i> = 105.185(3)° <i>c</i> = 17.029(2) Å <i>γ</i> = 90°	<i>a</i> = 13.6698(15) Å <i>α</i> = 90° <i>b</i> = 13.6698(15) Å <i>β</i> = 90° <i>c</i> = 32.116(5) Å <i>γ</i> = 90°
volume	3617.5(11) Å ³	4018.5(9) Å ³	6001.3(13) Å ³
<i>Z</i>	4	4	8
density (calcd)	1.502 Mg/m ³	1.539 Mg/m ³	1.546 Mg/m ³
absorp coeff	0.583 mm ⁻¹	0.664 mm ⁻¹	0.637 mm ⁻¹
<i>F</i> (000)	1660	1892	2824
cryst size	0.20 × 0.18 × 0.12 mm ³	0.20 × 0.18 × 0.14 mm ³	0.28 × 0.20 × 0.18 mm ³
<i>θ</i> range for data collection	2.02 to 27.54°	1.78 to 27.64°	2.11 to 27.55°
index ranges	-14 ≤ <i>h</i> ≤ 14, -20 ≤ <i>k</i> ≤ 21, -26 ≤ <i>l</i> ≤ 14	-20 ≤ <i>h</i> ≤ 15, -20 ≤ <i>k</i> ≤ 20, -19 ≤ <i>l</i> ≤ 22	-8 ≤ <i>h</i> ≤ 17, -17 ≤ <i>k</i> ≤ 17, -40 ≤ <i>l</i> ≤ 41
no. of reflns collected	24 107	27 053	40 691
no. of indep reflns	8314 [<i>R</i> (int) = 0.0326]	9278 [<i>R</i> (int) = 0.0676]	6920 [<i>R</i> (int) = 0.0537]
completeness to <i>θ</i> = 27.64°	99.5%	99.2%	99.5%
absorption correction	multiscans	multiscans	semiempirical from equivalents
max. and min. transmn	0.9333 and 0.8923	0.9128 and 0.8787	0.8939 and 0.8418
refinement method	full-matrix least-squares on <i>F</i> ²	full-matrix least-squares on <i>F</i> ²	full-matrix least-squares on <i>F</i> ²
no. of data/restraints/params	8314/38/473	9278/24/503	6920/10/417
goodness-of-fit on <i>F</i> ²	1.015	1.051	1.058
final <i>R</i> indices [<i>I</i> > 2σ(<i>I</i>)]	<i>R</i> 1 = 0.0469, <i>wR</i> 2 = 0.1201	<i>R</i> 1 = 0.0584, <i>wR</i> 2 = 0.1305	<i>R</i> 1 = 0.0489, <i>wR</i> 2 = 0.1293
<i>R</i> indices (all data)	<i>R</i> 1 = 0.0734, <i>wR</i> 2 = 0.1338	<i>R</i> 1 = 0.1305, <i>wR</i> 2 = 0.1488	<i>R</i> 1 = 0.0711, <i>wR</i> 2 = 0.1418
largest diff peak and hole	0.894 and -0.454 e Å ⁻³	0.836 and -0.745 e Å ⁻³	0.746 and -0.350 e Å ⁻³

Table 2. Selected Bond Distance (Å) and Angles (deg) for {TpRu[Ph₂CH₂P(O)Ph₂](OH)}BF₄ (2)

Interatomic Distances (Å)			
Ru(1)–O(1)	1.989(1)	Ru(1)–N(1)	2.033(2)
Ru(1)–N(3)	2.049(2)	Ru(1)–N(5)	2.107(1)
Ru(1)–P(1)	2.3224(6)	Ru(1)–O(2)	2.060(1)
P(2)–O(2)	1.528(1)	O(1)–H(1)	0.723(18)
Intramolecular Angles (deg)			
O(1)–Ru(1)–N(1)	95.16(5)	O(1)–Ru(1)–N(3)	174.69(5)
O(1)–Ru(1)–N(5)	87.83(6)	N(1)–Ru(1)–O(2)	172.72(5)
N(3)–Ru(1)–O(2)	89.89(6)	N(5)–Ru(1)–O(2)	86.53(5)
O(1)–Ru(1)–P(1)	87.11(3)	O(1)–Ru(1)–O(2)	89.20(5)
O(2)–Ru(1)–P(1)	87.34(4)	N(5)–Ru(1)–P(1)	172.03(4)
Ru(1)–O(1)–H(1)	110.3(14)		

generates a Ru^{III}-superoxo complex. A C–H bond of a methyl group of the Cp* ligand is then activated, giving rise to a monomeric hydrotetramethylfulvene complex, [Ru(η⁶-C₅Me₄CH₂)(tmed)(OH)]⁺.⁸ Also noteworthy is that several well-characterized superoxo complexes in the literature are supported by the sterically encumbered substituted hydrotri(pyrazolyl)borato ligands.¹¹ Many of these superoxo complexes show strong anti-ferromagnetic coupling between the metal center and the coordinated superoxide radical.^{11a–c,12} For example, it is evidenced that the effective magnetic moment (*μ*_{eff}) (295 K) = 2.8(1) μ_B of the chromium(III) superoxo

complex [Tp^{tBu,Me}Cr(pz'H)(O₂)]BAR₄ (Tp^{tBu,Me} = hydrotris(3-*tert*-butyl-5-methylpyrazolyl)borate; pz'H = 3-*tert*-butyl-5-methylpyrazole) results from strong antiferromagnetic coupling between the Cr^{III} ion (*d*³, *S* = 3/2) and the coordinated superoxide radical (*S* = 1/2).^{11a} The paramagnetic property of **4** indicates that such antiferromagnetic coupling is lacking for the complex.

[TpRu{Ph₂PCH₂CH₂P(=O)Ph₂}(OH)]BF₄ (6). The reaction of the dppp-dihydrogen complex [TpRu(dppp)(H₂)]BF₄ (**5**), generated in situ via HBF₄·OEt₂ acidification of TpRu(dppp)H in THF, with O₂ is similar to that of the dpmm analogue. Thus, the hydroxo complex [TpRu{Ph₂PCH₂CH₂CH₂P(=O)Ph₂}(OH)]BF₄ (**6**) was obtained as the major product contaminated by the aquo complex [TpRu(dppp)(H₂O)]BF₄ (**7**). The structure of **6** was determined by X-ray crystallography; the molecular structure of the cation **6**⁺ is shown in Figure 2. Crystal data and refinement details are given in Table 1. Selected bond distances and angles are given in Table 3. The Ru–OH distance (1.959(2) Å) in **6**⁺ is similar to that in **2**⁺. The Ru–O (phosphine oxide) bond distance, which is 2.069(2) Å, is also similar to that of **2**⁺. Like **2**, **6** was purified by recrystallization from CH₂Cl₂/hexanes. The pure complex, which is NMR silent, was characterized by IR spectroscopy, ESI-MS, and elemental analysis.

[TpRu^{III}(dppp)(O₂)]BF₄ (8). Similar to its dpmm analogue, reaction of the η²-dihydrogen complex [TpRu(dppp)(H₂)]BF₄, generated in situ in CH₂Cl₂, with O₂ yielded the superoxo complex [TpRu^{III}(dppp)(O₂)]BF₄ (**8**) as the major product contaminated with a minute amount of the aquo complex **7**, which could be removed by washing with diethyl ether and hexanes. Complex **8**

(11) (a) Qin, K.; Incarvito, C. D.; Rheingold, A. L.; Theopold, K. H. *Angew. Chem., Int. Ed.* **2002**, *41*, 2333. (b) Egan, J. W., Jr.; Haggerty, B. S.; Rheingold, A. L.; Sendlinger, S. C.; Theopold, K. H. *J. Am. Chem. Soc.* **1990**, *112*, 2445. (c) Fujisawa, K.; Tanaka, M.; Moro-oka, Y.; Kitajima, N. *J. Am. Chem. Soc.* **1994**, *116*, 12079. (d) Zhang, X.; Loppnow, G. R.; McDonald, R.; Takats, J. *J. Am. Chem. Soc.* **1995**, *117*, 7828.

(12) Cheung, S. K.; Grimes, C. J.; Wong, J.; Reed, C. A. *J. Am. Chem. Soc.* **1976**, *98*, 5028.

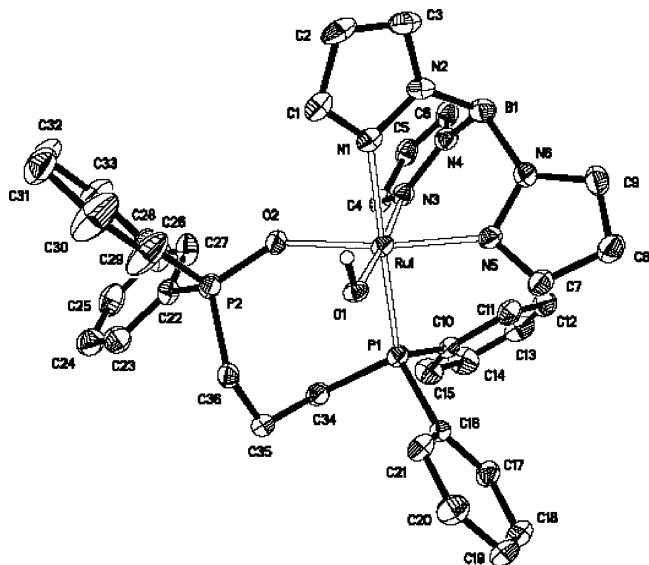


Figure 2. X-ray structure of $\{\text{TpRu}[\text{Ph}_2\text{P}(\text{CH}_2)_3\text{P}(\text{O})\text{Ph}_2](\text{OH})\}\text{BF}_4$ (**6**).

Table 3. Selected Bond Distance (Å) and Angles (deg) for $\{\text{TpRu}[\text{Ph}_2(\text{CH}_2)_3\text{P}(\text{O})\text{Ph}_2](\text{OH})\}\text{BF}_4$ (6**)**

Interatomic Distances (Å)			
Ru(1)–O(1)	1.959(2)	Ru(1)–N(1)	2.118(2)
Ru(1)–N(3)	2.033(2)	Ru(1)–N(5)	2.035(2)
Ru(1)–P(1)	2.3503(8)	Ru(1)–O(2)	2.069(2)
P(2)–O(2)	1.509(2)	O(1)–H(1A)	0.71(3)
Intramolecular Angles (deg)			
O(1)–Ru(1)–N(1)	88.70(8)	O(1)–Ru(1)–N(3)	174.10(8)
O(1)–Ru(1)–N(5)	91.63(9)	N(1)–Ru(1)–O(2)	88.25(9)
N(3)–Ru(1)–O(2)	87.17(9)	N(5)–Ru(1)–O(2)	173.53(8)
O(1)–Ru(1)–O(2)	91.02(8)	O(1)–Ru(1)–P(1)	92.99(5)
O(2)–Ru(1)–P(1)	92.15(6)	Ru(1)–O(1)–H(1A)	112(2)

was characterized by IR spectroscopy ($\nu(\text{O}_2^-) = 1191 \text{ cm}^{-1}$) and ESI-MS (m/z 759 (M^+) and m/z 727 [$\text{M} - \text{O}_2$] $^+$). Again, similar to the case of **4**, attempts to obtain single crystals of **8** for X-ray diffraction study were not successful.

Reaction of $[\text{TpRu}(\text{PPh}_3)_2(\text{H}_2)]\text{BF}_4$ (9**) with O_2 in THF.** Reaction of $[\text{TpRu}(\text{PPh}_3)_2(\text{H}_2)]\text{BF}_4$ (**9**), generated in situ in THF, with O_2 for 3 h afforded, after removal of the solvent, a reddish brown solid. Its $^{31}\text{P}\{^1\text{H}\}$ spectrum shows a major peak at δ 26.1 ppm, which is due to triphenylphosphine oxide $\text{Ph}_3\text{P}=\text{O}$, and a minor peak at δ 40.4 ppm, ascribable to the aquo complex $[\text{TpRu}(\text{PPh}_3)_2(\text{H}_2\text{O})]\text{BF}_4$ (**10**).⁷ After removal of the $\text{Ph}_3\text{P}=\text{O}$ from the reddish brown solid by washing with diethyl ether and hexanes, the proton NMR spectrum of the remaining solid was found to be identical to that of an authentic sample of **10**. The solid was recrystallized twice with $\text{CH}_2\text{Cl}_2/\text{hexanes}$. We suspect that similar to the formation of the dppm- and dppp-hydroxo complexes, **2** and **6**, respectively, the major component of the reddish brown solid is probably a paramagnetic hydroxo complex. A single crystal, obtained from the recrystallized solid, was subjected to an X-ray diffraction study. The molecular structure of the cation is shown in Figure 3. Crystal data and refinement details are given in Table 1. Selected bond distances and angles are given in Table 4. Although the hydrogen atoms of the two oxygen atoms cannot be located, we propose that the molecular structure of the crystal is that of an aquo-hydroxo species, $[\text{TpRu}(\text{PPh}_3)(\text{H}_2\text{O})(\text{OH})]\text{BF}_4$ (**11**). A

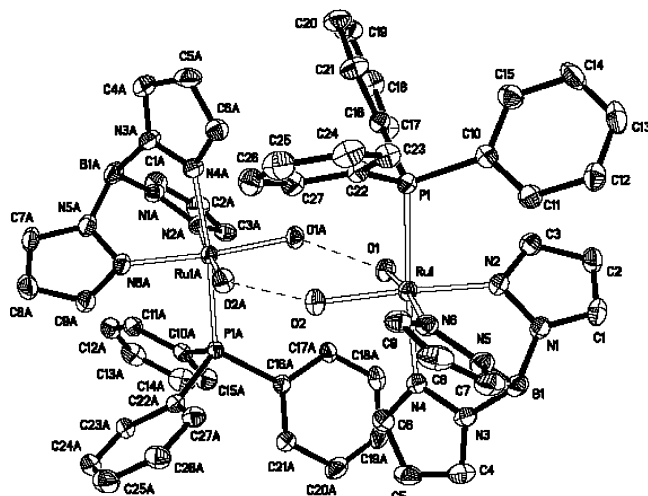


Figure 3. X-ray structure of $[\text{TpRu}(\text{PPh}_3)(\text{OH})(\text{H}_2\text{O})]\text{BF}_4$ (**11**).

Table 4. Selected Bond Distance (Å) and Angles (deg) for $[\text{TpRu}(\text{PPh}_3)(\text{OH})(\text{H}_2\text{O})]\text{BF}_4$ (11**)**

Interatomic Distances (Å)			
Ru(1)–O(2)	2.025(2)	Ru(1)–O(1)	2.0430(19)
Ru(1)–N(2)	2.035(2)	Ru(1)–N(4)	2.114(2)
Ru(1)–N(6)	2.046(2)	Ru(1)–P(1)	2.4181(8)
O(1)–O(1A)	2.523(7)	O(2)–O(2A)	2.487(7)
Intramolecular Angles (deg)			
O(2)–Ru(1)–N(2)	175.74(9)	O(2)–Ru(1)–N(4)	90.81(9)
O(2)–Ru(1)–N(6)	89.38(9)	O(2)–Ru(1)–P(1)	93.14(7)
O(1)–Ru(1)–N(2)	91.39(9)	O(1)–Ru(1)–N(4)	89.51(9)
O(1)–Ru(1)–N(6)	172.13(9)	O(1)–Ru(1)–P(1)	96.48(6)
O(2)–Ru(1)–O(1)	86.71(8)		

structural feature of **11**⁺ is the dimerization of the complex via the hydrogen-bonding interactions between the hydroxo group of one unit and the aquo ligand of another unit, as evidenced by the short O \cdots O distances (O1 \cdots O1A, 2.523(7) Å; O2 \cdots O2A, 2.487(7) Å). These distances are within the range of O \cdots O hydrogen bond distances in similar compounds.¹³ Dimerization via the formation of the intermolecular hydrogen bonds between the hydroxo and aquo groups has been reported for the vanadium complex $\text{Tp}^{\text{Pr}}\text{V}(\text{O})(\text{OH})(\text{H}_2\text{O})$ ^{13a} and the chromium species *cis*- $[\text{Cr}(\text{bpy})(\text{OH})(\text{H}_2\text{O})]_2$.^{4,13b} The elemental analysis of the recrystallized solid, however, did not agree with the molecular formula of **11**. In fact, several batches of the recrystallized solids obtained from independent experiments gave variable elemental analysis results, but none of them agreed with the molecular formula of **11**. We therefore suspect that complex **11** might be contaminated by other species, most probably the triphenylphosphine oxide complex $[\text{TpRu}(\text{PPh}_3)(\text{Ph}_3\text{P}=\text{O})(\text{OH})]\text{BF}_4$, which is the triphenylphosphine analogue of **2** and **6**.

$[\text{TpRu}^{\text{III}}(\text{PPh}_3)_2(\text{O}_2)]\text{BF}_4$ (12**).** Similar to its dppm and dppp analogues, reaction of **9** with O_2 in CH_2Cl_2 yielded the superoxo complex $[\text{TpRu}^{\text{III}}(\text{PPh}_3)_2(\text{O}_2)]\text{BF}_4$ (**12**) as the major product, the IR spectrum of which showed the superoxo band at 1190 cm^{-1} , and the ESI-

(13) (a) Kosugi, M.; Hikichi, S.; Akita, M.; Moro-oka, Y. *Inorg. Chem.* **1999**, *38*, 2567. (b) Ardon, M.; Bino, A. *Inorg. Chem.* **1985**, *24*, 1343. (c) Meyer, F.; Rutsch, P. *Chem. Commun.* **1998**, 1037. (d) Van Eldik, R.; Roodt, A.; Leipoldt, J. G. *Inorg. Chim. Acta* **1987**, *129*, L41. (e) Ghiladi, M.; Gomez, J. T.; Hazell, A.; Kofod, P.; Lumtscher, J.; McKenzie, C. J. *Dalton Trans.* **2003**, 1320. (f) Galsbøl, F.; Larsen, S.; Rasmussen, B.; Springborg, J. *Inorg. Chem.* **1986**, *25*, 290.

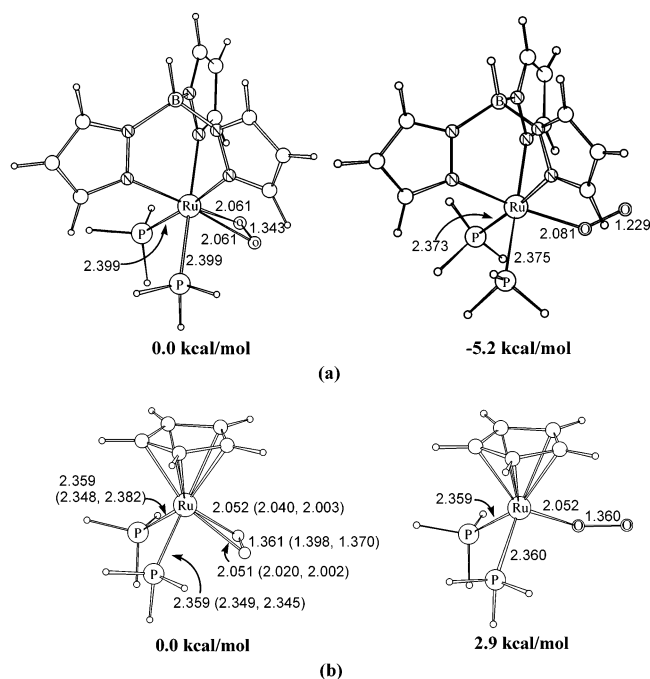


Figure 4. Calculated geometries for $\text{TpRu}(\text{PH}_3)_2(\text{O}_2)$ (a) and $\text{CpRu}(\text{PH}_3)_2(\text{O}_2)$ (b) in their singlet and triplet states. The structural parameters are given in Å. The values in parentheses were taken from the X-ray crystal structures of $[\text{Cp}^*\text{Ru}(\text{dppe})(\text{O}_2)]^+$ and $[\text{Cp}^*\text{Ru}(\text{dppe})(\text{O}_2)]^+$, respectively.

MS displayed the ions at m/z 871 and 839, corresponding to the parent ions $[\text{TpRu}(\text{PPh}_3)_2(\text{O}_2)]^+$ and $[\text{TpRu}(\text{PPh}_3)_2]^+$, respectively. Complex **12** was contaminated by a very small amount of the aquo complex **10** and a minute quantity of $\text{Ph}_3\text{P}=\text{O}$, which could be removed by washing with diethyl ether and hexanes. Similar to the other two superoxo complexes **4** and **8**, several attempts to obtain single crystals of **12** also met with failure.

Theoretical Study. To understand the preferential formation of the superoxo complexes $[\text{TpRu}(\text{L}_2)(\text{O}_2)]^+$, we examined the stability of the paramagnetic superoxo ruthenium(III) complex $[\text{TpRu}(\text{PPh}_3)_2(\text{O}_2)]^+$ (**12**⁺) theoretically. We carried out density functional theory calculations at the B3LYP level on the model complex $[\text{TpRu}(\text{PH}_3)_2(\text{O}_2)]^+$. The superoxo and the peroxy structures of the model complex were obtained through geometry optimization. The calculated geometries together with their relative energies are shown in Figure 4a. The $\eta^1\text{-O}_2$ superoxo complex is a triplet species in which antiferromagnetic coupling between the Ru(III) ion (d^5 , $S = 1/2$) and the coordinated superoxide radical ($S = 1/2$) seems to be lacking. As we tried to introduce such magnetic coupling to the system, it converted to the η^2 -peroxy structure, which is less stable than the η^1 -superoxo structure by 5.2 kcal/mol. The η^2 -peroxy complex has a formal Ru^{IV} metal center. These results provide additional support to the proposal that a formal ruthenium^{III}-superoxo complex $[\text{TpRu}(\text{L}_2)(\text{O}_2)]^+$ ($\text{L}_2 = \text{dpmm}$, dppp , or $(\text{PPh}_3)_2$) is responsible for its being NMR silent. The O–O bond distance (1.229 Å) in the superoxo structure is shorter than that in the peroxy structure (1.343 Å), due to the lesser back-donation from the metal center into the O–O π^* orbital of the superoxo ion.

To test the reliability of our theoretical calculations, we also carried out calculations on the analogous Cp model complex $[\text{CpRu}(\text{PH}_3)_2(\text{O}_2)]^+$. As mentioned above, the Cp ruthenium analogues normally adopt the η^2 -peroxy structure and have formally Ru^{IV} metal centers. The results of our calculations (see Figure 4b) indeed show that the η^2 -peroxy structure with a singlet state is more stable than the corresponding η^1 -superoxo structure with a triplet state. The calculated geometry of $[\text{CpRu}(\text{PH}_3)_2(\eta^2\text{-O}_2)]^+$ is also in good agreement with the relevant experimental ones of $[\text{Cp}^*\text{Ru}(\text{dppe})(\eta^2\text{-O}_2)]^+$ ^{2d} and $[\text{Cp}^*\text{Ru}(\text{dppm})(\eta^2\text{-O}_2)]^+$ ⁵.

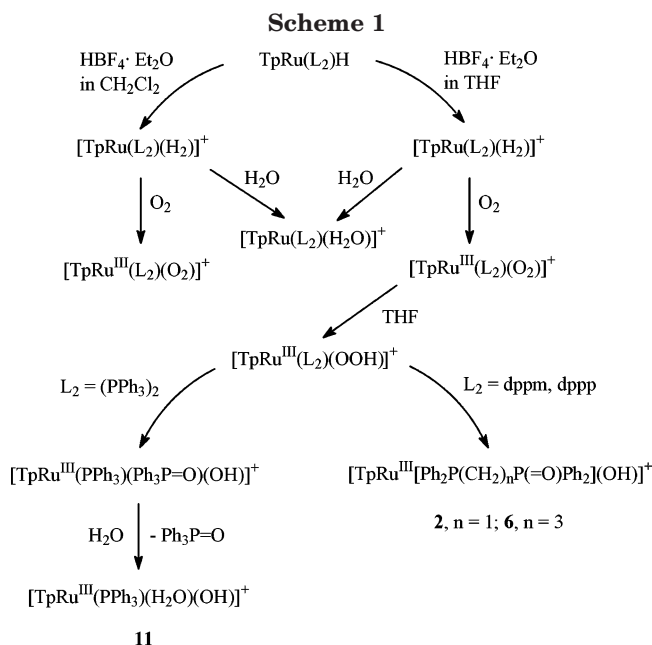
The different stability behavior between the Tp and Cp dioxygen complexes discussed above suggests that the Cp ligand is more electron-donating than the Tp ligand, although the relative electron-donating ability of Cp versus Tp is still controversial.¹⁴ In the complexes we studied here, it is likely that the more electron-donating Cp ligand stabilizes a Ru^{IV} center, while the weaker electron-donating Tp ligand prefers a metal center with a lower oxidation state. It is also possible that the more delocalized metal–ligand bonds made by Cp versus Tp play a role to stabilize the Ru^{IV} center. More studies are needed in order to thoroughly understand this issue. The results of our calculations suggest that Ru^{III} and a η^1 -superoxo ligand provide the optimal combination in the presence of a Tp ligand. We also calculated the analogous $\text{TpOs}(\text{PH}_3)_2(\text{O}_2)$ complex. As expected, the more electron-rich Os metal center stabilizes the $\eta^2\text{-O}_2$ coordination with a formal Os^{IV} metal center. The peroxy $\text{TpOs}(\text{PH}_3)_2(\eta^2\text{-O}_2)$ structure was calculated to be more stable by 1.7 kcal/mol than the superoxo $\text{TpOs}(\text{PH}_3)_2(\eta^1\text{-O}_2)$ structure. The different electronic properties of Tp and Cp have also been demonstrated in $[\text{CpRu}(\text{PPh}_3)_2\text{H}_2]^+$ ¹⁵ and $[\text{Tp}(\text{PPh}_3)_2\text{Ru}(\text{H}_2)]^+$,⁷ the former is a classical dihydride complex, while the latter is a nonclassical dihydrogen species. Also, our recent theoretical studies on the metathesis process $[\text{Tp}(\text{PH}_3)_2\text{Ru}(\text{R})(\eta^2\text{-H-CH}_3)] \rightarrow [\text{Tp}(\text{PH}_3)_2\text{Ru}(\text{CH}_3)(\eta^2\text{-H-R})]$ showed that the Tp-ruthenium species $\text{TpRu}(\text{PH}_3)_2(\text{R})(\text{H})(\text{Me})$ is only a transition state, while the corresponding reaction with the Cp complex passes through a formally Ru^{IV} intermediate, $\text{CpRu}(\text{PH}_3)_2(\text{H})(\text{Me})$.¹⁶

Proposed Reaction Mechanisms for Reactions of $[\text{TpRu}(\text{L}_2)(\text{H}_2)]^+$ with O_2 . The results of the reactions of the dihydrogen complexes $[\text{TpRu}(\text{L}_2)(\text{H}_2)]^+$, generated in situ in THF or CH_2Cl_2 , with O_2 can be interpreted in terms of the reaction sequence summarized in Scheme 1. The dihydrogen complex is readily generated through protonation of the hydride precursor; it is partially converted to the stable aquo complex $[\text{TpRu}(\text{L}_2)(\text{H}_2\text{O})]^+$ by reacting with the residual water in the solvent. In the CH_2Cl_2 solution, the superoxo complex is isolable, although it is contaminated with the aquo complex and probably a minute amount of the hydroxo complex (in the case of $[\text{TpRu}(\text{PPh}_3)_2(\text{O}_2)]^+$, by the additional $\text{Ph}_3\text{P}=\text{O}$). In THF, the superoxo complex

(14) (a) Sharp, P. R.; Bard, A. J. *Inorg. Chem.* **1983**, *22*, 2689. (b) Teller, D. M.; Skoog, S. J.; Bergman, R. G.; Gunnoe, T. B.; Harman, W. D. *Organometallics* **2000**, *19*, 2428. (c) Slugovc, C.; Padilla-Martínez, S. C.; Carmona, E. *Coord. Chem. Rev.* **2001**, *213*, 129. (d) Slugovc, C.; Schmid, R.; Kirchner, K. *Coord. Chem. Rev.* **1999**, *186*, 109.

(15) Wilczewski, T. *J. Organomet. Chem.* **1989**, *361*, 219.

(16) Lam, W. H.; Jia, G.; Lin, Z.; Lau, C. P.; Eisenstein, O. *Chem. Eur. J.* **2003**, *9*, 2775.



readily abstracts a hydrogen atom from the solvent molecule to form the hydroperoxo species $[\text{TpRu}(\text{L}_2)\text{-(OOH)}]^+$; the hydroperoxo ligand changes to the hydroxo group by transferring an oxygen atom to the phosphine ligand. It is well-documented that protonation of the O_2^{2-} ligand in peroxo complexes gives the hydroperoxo species,¹⁷ although the generation of hydroperoxo species via hydrogen atom abstraction by the O_2^- ligand in the superoxo complexes has also been implicated.^{6,18} It has been shown that treatment of the palladium hydroperoxo complex $(\text{Tp}^{i\text{Pr}_2})(\text{py})\text{Pd-OOH}$ with PPh_3 gives $\text{Ph}_3\text{P=O}$, and the resulting $(\text{Tp}^{i\text{Pr}_2})(\text{py})\text{Pd-OH}$ further condenses with $(\text{Tp}^{i\text{Pr}_2})(\text{py})\text{Pd-OOH}$, giving the $\mu\text{-}\kappa^1\text{:}\kappa^1\text{-peroxo}$ complex $(\text{Tp}^{i\text{Pr}_2})(\text{py})\text{Pd-OO-Pd}(\text{Tp}^{i\text{Pr}_2})\text{-(py)}$.¹⁹ Intramolecular O-transfer from the hydroperoxo ligand to the coordinated phosphine to generate phosphine oxide has been proposed in Jia's work⁵ and for the complex $(\text{PPh}_3)_2(\text{acac})\text{ClRh}(\text{OOH})$.²⁰ In our diphosphine complexes, one of the phosphine moieties of the diphosphine is oxidized to phosphine oxide and the resulting ligand remains bonded to the metal in a bidentate manner. For the triphenylphosphine complex, one of the PPh_3 ligands, which is oxidized to the phosphine oxide, is, however, displaced by H_2O to yield the aquo-hydroxo complex $[\text{TpRu}^{\text{III}}(\text{PPh}_3)(\text{H}_2\text{O})(\text{OH})]^+$.

Conclusion

This work provides some examples of Tp-supported superoxo (O_2^-) complexes. It shows that the Tp-ruthenium fragment $[\text{TpRu}(\text{L}_2)]^+$ ($\text{L}_2 = \text{dppm}$, dppp , or

$(\text{PPh}_3)_2$) is less electron-rich than the analogous Cp fragment $[\text{CpRu}(\text{L}_2)]^+$. The former reacts with O_2 to yield the η^1 -superoxo complex $[\text{TpRu}(\text{L}_2)(\eta^1\text{-O}_2)]^+$, in which the metal is a Ru^{III} center; the latter, on the other hand, undergoes reaction with O_2 to generate the η^2 -peroxo complex $[\text{CpRu}(\text{L}_2)(\eta^2\text{-O}_2)]$ with a formal Ru^{IV} metal center. The different electronic properties of Tp and Cp have also been demonstrated in the complexes $[\text{CpRu}(\text{PPh}_3)_2\text{H}_2]^+$ and $[\text{TpRu}(\text{PPh}_3)_2(\text{H}_2)]^+$.

Experimental Section

Ruthenium trichloride, $\text{RuCl}_3 \cdot 3\text{H}_2\text{O}$, pyrazole, and sodium borohydride were obtained from Aldrich. Triphenylphosphine was purchased from Merck and was recrystallized from ethanol before use. The complexes $\text{TpRu}(\text{dppm})\text{H}$, $\text{TpRu}(\text{dppp})\text{H}$, and $\text{TpRu}(\text{PPh}_3)_2\text{H}$ were synthesized according to published procedures.⁷ Solvents were distilled under a dry nitrogen atmosphere with appropriate drying agents: dichloromethane with calcium hydride, tetrahydrofuran, diethyl ether, and hexanes with sodium-benzophenone ketyl. High-purity hydrogen and oxygen gases were supplied by Hong Kong Oxygen.

Infrared spectra were obtained from a Bruker Vector 22 FT-IR spectrophotometer. Proton NMR spectra were obtained from a Bruker DPX 400 spectrometer at 400.13 MHz. Chemical shifts were reported relative to residual protons of the deuterated solvents. $^{31}\text{P}\{^1\text{H}\}$ NMR spectra were recorded on a Bruker DPX 400 spectrometer at 161.70 MHz; the chemical shifts were externally referenced to 85% H_3PO_4 in D_2O . Electrospray ionization mass spectrometry was carried out with a Finnigan MAT 95S mass spectrometer with the samples dissolved in $\text{CH}_2\text{Cl}_2/\text{MeOH}$. Elemental analyses were performed by M-H-W Laboratories, Phoenix, AZ.

$[\text{TpRu}\{\text{Ph}_2\text{PCH}_2\text{P}(\text{=O})\text{Ph}_2\}(\text{OH})\text{BF}_4$ (2). A sample of $\text{TpRu}(\text{dppm})\text{H}$ (0.10 g, 0.12 mmol) was dissolved in THF (10 mL) in a Schlenk flask. $\text{HBF}_4 \cdot \text{Et}_2\text{O}$ (54%, 19 μL , 1.15 equiv) was added to the solution, and it was stirred at room temperature for 1 h. The resulting solution was then subjected to 1 atm of O_2 for 3 h, during which the color of the solution changed from yellow to reddish brown. The solvent was removed under vacuum to afford a reddish brown solid, which was recrystallized from $\text{CH}_2\text{Cl}_2/\text{hexanes}$ to yield the pure complex. Yield: 0.083 g (85%). Anal. Calcd for $\text{C}_{34}\text{H}_{33}\text{B}_2\text{F}_4\text{N}_6\text{O}_2\text{-P}_2\text{Ru}$: C, 49.90; H, 4.06. Found: C, 49.88; H, 4.04. IR (KBr, cm^{-1}): $\nu(\text{OH})$ 3127 (w), $\nu(\text{P=O})$ 1118 (sh). ESI-MS ($\text{CH}_2\text{Cl}_2/\text{MeOH}$): m/z 732 $[\text{M} - \text{BF}_4]^+$.

$[\text{TpRu}(\text{dppm})(\text{H}_2\text{O})\text{BF}_4$ (3). A sample of $\text{TpRu}(\text{dppm})\text{H}$ (0.10 g, 0.14 mmol) was dissolved in THF (8 mL) in a Schlenk flask. $\text{HBF}_4 \cdot \text{Et}_2\text{O}$ (54%, 22 μL , 1.1 equiv) was added to the solution, and it was stirred at room temperature for 1 h. Water (25 μL , 10 equiv) was then added to the resulting solution, which was stirred at room temperature for an hour. Solvent was removed under vacuum to afford a light yellow solid, which was washed with diethyl ether (2 \times 3 mL) and hexanes (2 \times 2 mL) and dried under vacuum. Yield: 0.093 g (83%). Anal. Calcd for $\text{C}_{34}\text{H}_{34}\text{B}_2\text{F}_4\text{N}_6\text{OP}_2\text{Ru}$: C, 50.84; H, 4.27. Found: C, 50.62; H, 4.29. ^1H NMR (400.13 MHz, CD_2Cl_2 , 25 $^\circ\text{C}$): δ 2.58 (s, 2H, H_2O), 4.93 (m, 2H, PCH_2P), 5.42 (1H of Tp), 6.05 (1H of Tp), 6.37 (2H of Tp), 7.65 (2H of Tp), 7.68 (1H of Tp), 7.96 (2H of Tp), 6.96–7.63 (m, 20 H of phenyl rings of dppm). $^{31}\text{P}\{^1\text{H}\}$ NMR (161.70 MHz, CD_2Cl_2 , 25 $^\circ\text{C}$): 3.3 (s).

$[\text{TpRu}^{\text{III}}(\text{dppm})(\text{O}_2)\text{BF}_4$ (4). A sample of $\text{TpRu}(\text{dppm})\text{H}$ (0.10 g, 0.14 mmol) was dissolved in CH_2Cl_2 (10 mL) in a Schlenk flask. $\text{HBF}_4 \cdot \text{Et}_2\text{O}$ (54%, 19 μL , 1.15 equiv) was added to the solution, and it was stirred at room temperature for 1 h. The solution was then stirred under 1 atm of O_2 for 3 h, leading to the formation of a red solution. The solvent was removed to afford a red solid, which was washed with diethyl ether (2 \times 5 mL) and hexanes (2 \times 5 mL) and dried under

(17) (a) Conte, V.; Di Furia, F.; Moro, S. *J. Mol. Catal. A: Chem.* **1997**, *120*, 93. (b) Ho, R. Y. N.; Roelfes, G.; Hermant, R.; Hage, R.; Feringa, B. L.; Que, L., Jr. *Chem. Commun.* **1999**, 2161. (c) Takahashi, Y.; Hashimoto, M.; Hikichi, S.; Akita, M.; Moro-oka, Y. *Angew. Chem., Int. Ed.* **1999**, *38*, 3074. (d) Suzuki, H.; Matsunra, S.; Moro-oka, Y.; Ikawa, T. *Chem. Lett.* **1982**, 1011. (e) Carmona, D.; Lamata, M. P.; Ferrer, J.; Modrego, J.; Perales, M.; Lahoz, F. J.; Atencio, R.; Oro, L. A. *J. Chem. Soc., Chem. Commun.* **1994**, 575. (f) Konnick, M. M.; Guzei, I. A.; Stahl, S. S. *J. Am. Chem. Soc.* **2004**, *126*, 10212.

(18) Wick, D. D.; Goldberg, K. I. *J. Am. Chem. Soc.* **1999**, *121*, 11900.

(19) Miyaji, T.; Jujime, M.; Hikichi, S.; Moro-oka, Y.; Akita, M. *Inorg. Chem.* **2002**, *41*, 5286.

(20) Suzuki, H.; Matsunra, S.; Moro-oka, Y.; Ikawa, T. *J. Organomet. Chem.* **1985**, *286*, 247.

vacuum. Yield: 0.080 g (~82%). Anal. Calcd for $C_{34}H_{32}B_2F_4N_6O_2$ - P_2Ru : C, 49.97; H, 3.95. Found: C, 49.43; H, 4.13. IR (KBr, cm^{-1}): $\nu(O_2^-)$ 1191 (w). ESI-MS (CH_2Cl_2): m/z 731 [M - BF_4] $^+$.

[TpRu{Ph₂PCH₂CH₂CH₂P(=O)Ph₂}(OH)]BF₄ (6). Complex **6** was prepared by using the same procedure as for the preparation of **2** except that TpRu(dppp)H was used in place of TpRu(dppm)H. Yield: 0.084 g (83%). Anal. Calcd. for $C_{36}H_{37}B_2F_4N_6O_2P_2Ru$: C, 51.09; H, 4.41. Found: C, 51.26; H, 4.39. IR (KBr, cm^{-1}): $\nu(OH)$ 3116 (w), $\nu(P=O)$ 1123 (sh). ESI-MS ($CH_2Cl_2/MeOH$): m/z 760 [M - BF_4] $^+$.

[TpRu(dppp)(H₂O)]BF₄ (7). Complex **7** was prepared using the same procedure as for the preparation of **3** except that TpRu(dppp)H was used instead of TpRu(dppm)H. Yield: 0.093 g (80%). Anal. Calcd for $C_{36}H_{38}B_2F_4N_6O_2P_2Ru$: C, 52.01; H, 4.61. Found: C, 52.37; H, 4.60. ¹H NMR (400.13 MHz, $CDCl_3$, 25 °C): δ 2.28 (m, 2H of $PCH_2CH_2CH_2P$), 2.50 (s, 2H, H_2O), 2.88 (m, 2H of $PCH_2CH_2CH_2P$), 3.09 (m, 2H of $PCH_2CH_2CH_2P$), 5.00 (H of Tp), 5.46 (1H of Tp), 5.99 (2H of Tp), 6.33 (2H of Tp), 6.92–7.55 (m, 20H of phenyl groups of dppp), 6.94 (1H of Tp), 7.96 (2H of Tp). ³¹P{¹H} NMR (161.99 MHz; CD_2Cl_2 , 25 °C): δ 31.1 (s).

[TpRu^{III}(dppp)(O₂)]BF₄ (8). Complex **8** was prepared using the same procedure as for the preparation of **4** except that TpRu(dppp)H was used in place of TpRu(dppm)H. Yield: 0.085 g (~84%). Anal. Calcd for $C_{36}H_{36}B_2F_4N_6O_2P_2Ru$: C, 51.15; H, 4.29. Found: C, 50.95; H, 4.20. IR (KBr, cm^{-1}): $\nu(O_2^-)$ 1192 (w). ESI-MS ($CH_2Cl_2/MeOH$): m/z 959 [M - BF_4] $^+$.

[TpRu(PPh₃)(H₂O)(OH)]BF₄ (11). Complex **11** was prepared using the same procedure as for the preparation of **3** except that TpRu(PPh₃)₂H was used instead of TpRu(dppm)H. Yield: 0.072 g (86%). IR (KBr, cm^{-1}): $\nu(OH)$ 3127 (w). ESI-MS ($CH_2Cl_2/MeOH$): m/z 594 [M - H_2O - BF_4] $^+$.

[TpRu^{III}(PPh₃)₂(O₂)]BF₄ (12). Complex **12** was prepared using the same procedure as for the preparation of **4** except that TpRu(PPh₃)₂H was used instead of TpRu(dppm)H. Yield: 0.079 g (~80%). Anal. Calcd for $C_{45}H_{40}B_2F_4N_6O_2P_2Ru$: C, 56.45; H, 4.21. Found: C, 56.38; H, 4.31. IR (KBr, cm^{-1}): $\nu(O_2^-)$ 1190 (w). ESI-MS ($CH_2Cl_2/MeOH$): m/z 871 [M - BF_4] $^+$.

Crystallographic Studies. Crystals of **2**, **6**, and **11** suitable for X-ray diffraction studies were obtained by layering of hexane on CH_2Cl_2 solutions of these complexes. A suitable crystal of each of the complexes was mounted on a Bruker CCD area detector diffractometer using Mo $K\alpha$ radiation ($\lambda = 0.71073$ Å) from a generator operating at 50 kV, 30 mA condition. The intensity data of **2**, **6**, and **11** were collected in the range of $2\theta = 3$ – 55° , with oscillation frames of ϕ and ω in the range 0– 180° . Frames of 1321 were taken in 4 shells. An empirical absorption correction of the SADABS (Sheldrick, 1996) program based on Fourier coefficient fitting was applied. The crystal structures were determined by the direct method, yielding the positions of part of the non-hydrogen atoms, and subsequent difference Fourier syntheses

were employed to locate all the non-hydrogen atoms that did not show up in the initial structure. Hydrogen atoms were located based on difference Fourier syntheses connecting geometrical analysis. All non-hydrogen atoms were refined anisotropically with weight function $w = 1/[\sigma^2(F_o^2) + 0.1000p]^2 + 0.0000p]$, where $p = (F_o^2 + 2F_c^2)/3$ were refined. Hydrogen atoms were refined with fixed individual displacement parameters. All experiments and computations were performed on a Bruker CCD area detector diffractometer and PC computer with the Bruker Smart and Bruker SHELXT1 program packages.

Computational Details. In the B3LYP density functional theory calculation, the Stuttgart/Dresden effective core potentials and basis sets²¹ were used to describe Ru, while the standard 6-31G basis set was used for C, P, O, and H atoms. Polarization functions ($\zeta(d) = 0.6$) were added for all the carbons, ($\zeta(d) = 0.34$) for the phosphine ligand, and ($\zeta(d) = 1.154$) for the oxygens.²² Frequency calculations at the same level of theory have also been performed to confirm all the stationary points. All the calculations were performed with the Gaussian 98 software package.²³

CCDC reference numbers 238295–238297

Acknowledgment. We thank the Hong Kong Research Grant Council (Project No. PolyU5188/00P) and the Hong Kong Polytechnic University for financial support.

Supporting Information Available: Tables of X-ray structural data, including data collection parameters, positional and thermal parameters, and bond distances and angles, for complexes **2**, **6**, and **11**. This material is available free of charge via the Internet at <http://pubs.acs.org>.

OM0494030

(21) (a) Haeusermann, U.; Dolg, M.; Stoll, H. Preuss, H. *Mol. Phys.* **1993**, *78*, 1211. (b) Kuechle, W.; Dolg, M.; Stoll, H.; Preuss, H. *J. Chem. Phys.* **1994**, *100*, 7535. (c) Leininger, T.; Nicklass, A.; Stoll, H.; Dolg, M.; Schwerdtfeger, P. *J. Chem. Phys.* **1996**, *105*, 1052.

(22) Huzinaga, S. *Gaussian Basis Sets for Molecular Calculations*; Elsevier Science Pub. Co.: Amsterdam, 1984.

(23) Frisch, M. J.; Trucks, G. W.; Schlegel, H. B.; Scuseria, G. E.; Robb, M. A.; Cheeseman, J. R.; Zakrzewski, V. G.; Montgomery, J. A., Jr.; Stratmann, R. E.; Burant, J. C.; Dapprich, S.; Millam, J. M.; Daniels, A. D.; Kudin, K. N.; Strain, M. C.; Farkas, O.; Tomasi, J.; Barone, V.; Cossi, M.; Cammi, R.; Mennucci, B.; Pomelli, C.; Adamo, C.; Clifford, S.; Ochterski, J.; Petersson, G. A.; Ayala, P. Y.; Cui, Q.; Morokuma, K.; Malick, D. K.; Rabuck, A. D.; Raghavachari, K.; Foresman, J. B.; Cioslowski, J.; Ortiz, J. V.; Stefanov, B. B.; Liu, G.; Liashenko, A.; Piskorz, P.; Komaromi, I.; Gomperts, R.; Martin, R. L.; Fox, D. J.; Keith, T.; Al-Laham, M. A.; Peng, C. Y.; Nanayakkara, A.; Gonzalez, C.; Challacombe, M.; Gill, P. M. W.; Johnson, B. G.; Chen, W.; Wong, M. W.; Andres, J. L.; Head-Gordon, M.; Replogle, E. S.; Pople, J. A. *Gaussian 98*, revision A.9; Gaussian, Inc.: Pittsburgh, PA, 1998.